Image compression based on periodic principal components

Wilmar Hernandez[1]
Facultad de Ingenieria y Ciencias Aplicadas
Universidad de Las Americas, Ecuador
Email: wilmar.hernandez@udla.edu.ec

Alfredo Mendez[2]
Departamento de Matematica Aplicada
a las Tecnologias de la Informacion y Comunicaciones
Universidad Politecnica de Madrid, Spain
Email: alfredo.mendez@upm.es

Pablo Alejandro Quezada-Sarmiento[3]
Tecnologia en Redes y Telecomunicaciones
Instituto Tecnologico Superior Daniel Alvarez Burneo, Ecuador
Email: paquezada@itsmaristaloja.edu.ec

Luis Alberto Jumbo-Flores[4]
Escuela de Informatica y Multimedia
Universidad Internacional del Ecuador, Ecuador
Email: luis.jumbo.alberto@gmail.com

Paolo Mercorelli[5]
Control and Drive Systems Laboratory
Leuphana University of Lüneburg, Germany
Email: mercorelli@uni.leuphana.de

Vera Tyrsa[6]
Instituto de Ingeniera
Universidad Autonoma de Baja California, Mexico
Email: vtyrsa@uabc.edu.mx

Patricia Acosta-Vargas[7]
Intelligent & Interactive Systems Lab
Universidad de Las Americas, Quito, Ecuador
Email: patricia.acosta@udla.edu.ec

Ivan Menes Camejo[8]
Facultad de Informatica y Electronica
Escuela Superior Politecnica de Chimborazo, Ecuador
Email: imenes@espoch.edu.ec

Jose Rigoberto Muñoz Cagua[9]
Centro de Investigacion de Energias Alternativas y Ambiente
Escuela Superior Politecnica de Chimborazo, Ecuador
Email: jmunoz@espoch.edu.ec

Willam Bladimir Cevallos Cevallos[10]
Escuela Superior Politecnica de Chimborazo, Ecuador
Email: willambladimir@hotmail.es

***Abstract*—In the present paper, the almost periodicity of the first principal components is studied, with the aim of being able to use less information in order to obtain acceptable reconstructions of compressed images. The results of this study show that by working with the periodic principal components of images under analysis, it is possible to obtain an additional reduction to that obtained by using the original principal components. Specifically, it is shown that if the principal components that are considered periodic are replaced by their period plus a trend, it can be said that the reconstruction achieved using these periodic principal components is very close to the reconstruction achieved using the original principal components.**

I. Introduction

Principal component analysis (PCA), also known as the Hotelling transform or Karhunen-Loeve transform, is a statistical technique that was proposed by Karl Pearson (1901) as part of factorial analysis; however, its first theoretical development appeared in 1933 in a paper written by Hotelling [1]–[4]. The complexity of the calculations involved in this technique delayed its development until the birth of computers, and its effective use started in the second half of the 20th century.

This technique allows to transform multidimensional data sets into spaces of lower dimensions, minimizing the loss of original information. With this procedure there is a new set of orthogonal axes that are forming low-dimensional vector subspaces and on which the set of points is projected so that the variance of these projections is maximum [5]. By having p variables collected on the units analyzed, all are required to reproduce the total variability of the system, and sometimes most of that variability can be found in a small number, k, of principal components. Its origin lies in the redundancy that there is many times between different variables. Thus redundancy is data, not information. For real world images, the dependence of a pixel with its neighbors is clear, so there is a dependence on location. The k principal components can replace the p initial variables, so that the original set of data, consisting of n measures of p variables, is reduced to n measures of k principal components [5].

PCA is among the most acclaimed multivariate statistical techniques and it is used by a wide range of scientific disciplines [6]. For example, in [7], a method to locate the optic disk automatically is proposed and PCA is applied to

978-1-7281-4878-6/19/$31.00 ©2019 IEEE

candidate regions, which are first determined by clustering the brightest pixels. This is an example of PCA techniques applied to object detection. A literature review on the use of PCA for face recognition, face verification, automatic location of optic disk in retinal images, and texture analysis is carried out in [8]. Also, in [9] PCA is used in image noise cancellation.

In addition, examples of application of PCA techniques to object tracking can be found in [10], [11]. The examples of applications of PCA techniques shown in [12]–[14] are aimed at traffic control systems. In [15], [16], PCA techniques are used for three-dimensional reconstruction, and some applications of PCA techniques to forms recognition can be found in [17]–[20]. Finally, in [21] PCA techniques are used for image compression. In that paper, the problem of bandwidth consumption over multimedia communication is addressed, and it is made clear that having an effective compression coding scheme with low bit rates is crucial to enable the effective and fast transmission of image data over the network.

The present paper is aimed at studying the almost periodicity of the first principal components, with the aim of being able to use less information in order to obtain acceptable reconstructions of compressed images. Furthermore, it is shown that by doing this we can achieve an additional reduction to that obtained through the use of the original principal components.

II. Methodology used for image compression

Geometrically, the data are n points of $\mathbb{R}^p$ and the principal components represent an orthogonal transformation, whose coordinate axes are the axes of the ellipsoid E_p and with lengths proportional to $\sqrt{\hat{\lambda}_i}$, being $\hat{\lambda}_i$ the eigenvalues of either the variance/covariance matrix or the correlation matrix. Since all eigenvectors can be chosen of norm equal to 1, the absolute value of the i-th component $|\hat{y}_i| = |\hat{\mathbf{e}}_i^t\,(\mathbf{x}-\bar{\mathbf{x}})|$ is the length of the projection of the vector $(\mathbf{x}-\bar{\mathbf{x}})$ on the vector $\hat{\mathbf{e}}_i$. Therefore, the principal components can be seen as a translation of the origin to the point $\bar{\mathbf{x}}$ and a rotation of the axes until they pass through the directions with greatest variability.

When there is a high positive correlation between all the variables and a principal component with all its coordinates of the same sign, this component can be considered as a weighted average of all the variables, or the size of the index that forms that component. The components that have coordinates of different sign oppose a subset of variables against another, being a weighted average of two groups of variables.

In this paper, a set of six gray images (known as Barbara, Fig. 1; Boats, Fig. 2; Goldhill, Fig. 3; Lena, Fig. 4; Mandrill, Fig. 5, and Peppers, Fig. 6) will be considered, which consists of images that have been widely used in the literature on image processing. Here, the gray scale versions of size 512×512 have been taken into account.

Given an image of those considered, we partition the image (1) and subdivide it into non-overlapping cells of size $2^n \times 2^n = k^2$, $\mathbf{A}_{ij}$, with what we obtain $2^{9-n} \cdot 2^{9-n} = h^2$ blocks, and each of them will be a vector of observations.

Fig. 1. Barbara.

Fig. 2. Boats.

Fig. 3. Goldhill.

Fig. 4. Lena.

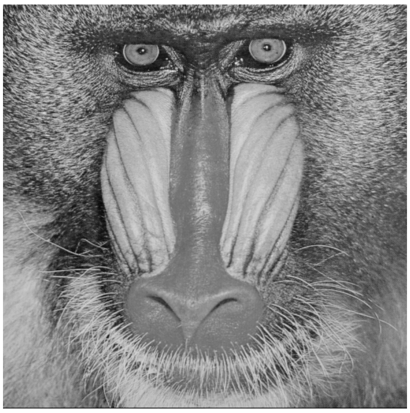

Fig. 5. Mandrill.

Fig. 6. Peppers.

$$\mathbf{Image} = \begin{bmatrix} \mathbf{A}_{1,1} & \dots & \mathbf{A}_{1,h} \\ \vdots & \ddots & \vdots \\ \mathbf{A}_{h,1} & \dots & \mathbf{A}_{h,h} \end{bmatrix} \tag{1}$$

Now, each matrix $\mathbf{A}_{ij}$ is stored in a vector of dimension k^2, $\mathbf{x}$, which contains the elements of the matrix by rows, that is to say $\mathbf{x} = [a_{i,1}, \dots, a_{i,k}, a_{i+1,1}, \dots, a_{i+1,k}, \dots, a_{i+k,k}]$. In this way we have the observations $\{\mathbf{x}_\ell \in \mathbb{R}^{k^2} \mid \ell = 1, \dots, h^2\}$, which we group in the observations matrix $\mathbf{x} = (x_{ij}) \in \mathcal{M}_{h^2, j^2}(\mathbb{R})$. Then, we find the k^2 pairs of eigenvalues and eigenvectors, $(\hat{\lambda}_i, \hat{\mathbf{e}}_i)$, with $\hat{\mathbf{e}}_i$, and order them according to the eigenvalues from highest to lowest.

In general, the first eigenvalue is much larger than the rest, so that the first principal component fully dominates the total variability. Therefore, the k^2 principal components $\hat{y}_j = \hat{\mathbf{e}}_j^t \mathbf{x} = \hat{e}_{1,j} x_1 + \dots + \hat{e}_{k^2,j} x_p$, with $j = 1, \dots, p$, have been built and consequently we have an orthonormal basis, $B' = \{\hat{\mathbf{e}}_1, \dots, \hat{\mathbf{e}}_{k^2}\}$, of $\mathbb{R}^{k^2}$. Each vector $\hat{\mathbf{e}}_j = [\hat{e}_{1,j}, \dots, \hat{e}_{k^2,j}]^t$ is grouped by rows in an $\mathcal{M}_{k,k}$ matrix (2).

$$\hat{\mathbf{E}}_j = \begin{bmatrix} \hat{e}_{1,j} & \dots & \hat{e}_{k,j} \\ \vdots & \ddots & \vdots \\ \hat{e}_{k^2-k+1,j} & \dots & \hat{e}_{k^2,j} \end{bmatrix} \tag{2}$$

Given a vector $\mathbf{v}$ that with respect to the canonical base has coordinates $(x_1, \dots, x_{k^2})$ and with respect to the base B' its coordinates are $(y_1, \dots, y_{k^2})$, the relation between these coordinates is $(x_1, \dots, x_{k^2})^t = \mathbf{CP}(y_1, \dots, y_{k^2})^t$. Also, since the matrix $\mathbf{CP}$ is orthogonal, it has to be $(y_1, \dots, y_{k^2}) = (x_1, \dots, x_{k^2})\mathbf{CP}$. So, the coordinates of the h^2 vectors that form the observation matrix have as coordinates, with respect to the new base, the rows of the matrix with dimension $h^2 \times k^2$ given by $\mathbf{y} = \mathbf{x} \cdot \mathbf{CP}$.

If we keep all the B' vectors, we can perfectly reconstruct our data matrix, because $\mathbf{y} = \mathbf{x} \cdot \mathbf{CP}$ implies $\mathbf{x} = \mathbf{y} \cdot \mathbf{CP}^{-1} = \mathbf{y} \cdot \mathbf{CP}^t$.

To compress the image, we are left with the first vectors of the base B', that is to say that we still have vectors each of them with k^2 components, but we have only h^2 vectors, with $h < k$. If we stay with M components, $M < k^2$, we define the matrix (3) of order $k^2 \times k^2$, which in the upper left corner has a block formed by the identity matrix of order M and the rest of the elements are zero.

$$\mathbf{T}_M = \begin{bmatrix} \mathbf{I}_{M \times M} & \mathbf{0}_{M \times (k^2-M)} \\ \mathbf{0}_{(k^2-M) \times M} & \mathbf{0}_{(k^2-M) \times (k^2-M)} \end{bmatrix} \tag{3}$$

Therefore, the matrix $\mathbf{y}_M = \mathbf{y} \cdot \mathbf{T}_M = \mathbf{x} \cdot \mathbf{CP} \cdot \mathbf{T}_M$ has the same dimension as the observations matrix $h^2 \times k^2$, but where the last $(k^2 - M)$ columns are all zero, that is, we have reduced the dimension $h^2 \times k^2$ to $h^2 \times M$ and the rest has been filled with zeros.

To reconstruct the compressed image, the inverse operations are carried out, that is to say, each row of $\mathbf{y}_M$ is reordered in a $k \times k$ matrix, so the i-th row of $\mathbf{y}_M$ is transformed into the matrix given by (4), with $i = 1, \dots, h^2$.

$$\mathbf{B}_i = \begin{bmatrix} b_{i,1} & \cdots & b_{i,k} \\ b_{i,\,k+1} & \cdots & b_{i,2\cdot k} \\ \vdots & \ddots & \vdots \\ b_{i,\,k^2-k+1} & \cdots & b_{i,\,k^2} \end{bmatrix} \quad (4)$$

Now, we build the compressed image matrix (5) of dimension 512×512 formed by $k^2 \times k^2$ blocks, each block being a $\mathbf{B}_i$ matrix.

$$\mathbf{Image}_{comp} = \begin{bmatrix} \mathbf{B}_1 & \dots & \mathbf{B}_{k^2} \\ \mathbf{B}_{k^2+1} & \dots & \mathbf{B}_{2\cdot k^2} \\ \vdots & \ddots & \vdots \\ \mathbf{B}_{h^2-k^2+1} & \dots & \mathbf{B}_{h^2} \end{bmatrix} \quad (5)$$

In order to correctly predict the quality that is really appreciated by the observer, the method we will use is the peak signal-to-noise ratio (PSNR). The PSNR measure evaluates the quality in terms of deviations between the processed image and the original, that is, an error value. If the pixels of the original image are $\{x_n,$ with $n = 1, \dots, N\}$, with N being the number of rows by the number columns of the image, the pixels of the reconstruction are $\{y_n,$ with $n = 1, \dots, N\}$, the error is the difference $\{r_n = x_n - y_n,$ with $n = 1, \dots, N\}$, and we consider the mean squared error (MSE) of (r_n), then $MSE = \frac{1}{N} \sum_{i=1}^{N} r_n^2$.

A measure of the quality of the image is the rate between the variance of the signal and the variance of the error (measured in dB), when the signal is a discrete variable the variability in the original image is replaced by the squared of the maximum value of the signal, obtaining the PSNR. In the case of 8-bit images, the PSNR of the reconstruction is given by (6).

$$\text{PSNR} = 10\ \log_{10}\left(\frac{(2^8-1)^2}{MSE}\right) = 10\ \log_{10}\left(\frac{255^2}{MSE}\right) \quad (6)$$

We have already mentioned, in previous paragraphs, that the first eigenvalue is much larger than the rest, and that the first principal component completely dominates the total variability. Thus, the k^2 principal components $\hat{y}_j = \hat{\mathbf{e}}_j^t\,\mathbf{x} = \hat{e}_{1,j}\,x_1 + \ldots + \hat{e}_{k^2,j}\,x_p$, with $j = 1, \dots, p$, have been built, and therefore we have an orthonormal basis, $B' = \{\hat{\mathbf{e}}_1, \dots, \hat{\mathbf{e}}_{k^2}\}$, of $\mathbb{R}^{64}$. Each vector $\hat{\mathbf{e}}_j = [\hat{e}_{1,j}, \dots, \hat{e}_{64,j}]^t$ is grouped by rows in an $\mathcal{M}_{8,\,8}$ matrix (see (2)).

In practice, the periodic behavior of the coordinates, in the canonical basis, of the vectors of the base B' can be observed. The explanation is that there is a dependency of a pixel in relation to its neighbors and that when we have $k \times k$ submatrices, which we have stored by rows in a vector, the values of one pixel of that submatrix are quite similar to those of another pixel that is separated of this by k elements of the vector that we have formed. In Figs. 7, 8, 9, 10, 11, and 12 we have included the first principal component of the considered images. For the images of Figs. 1, 2 and 3, $2^4 \times 2^4$ cells have been considered; and for images of Figs. 4, 5, and 6, $2^5 \times 2^5$ cells been considered.

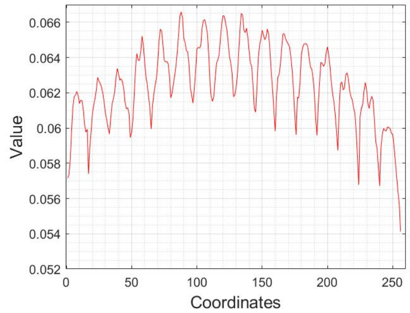

Fig. 7. Coefficients of the first principal component: Barbara.

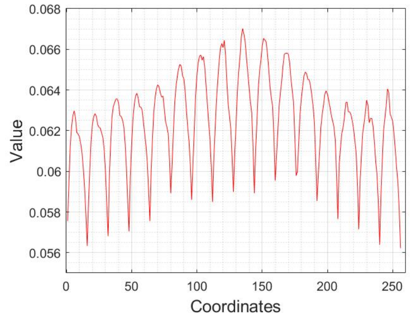

Fig. 8. Coefficients of the first principal component: Boats.

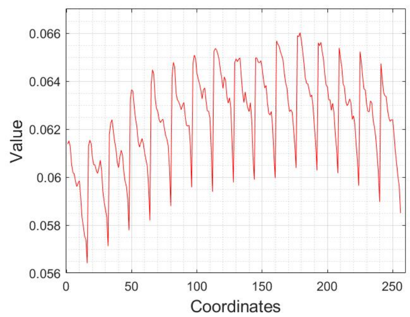

Fig. 9. Coefficients of the first principal component: Goldhill.

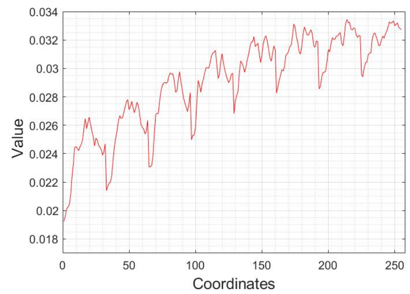

Fig. 10. Coefficients of the first principal component: Lena.

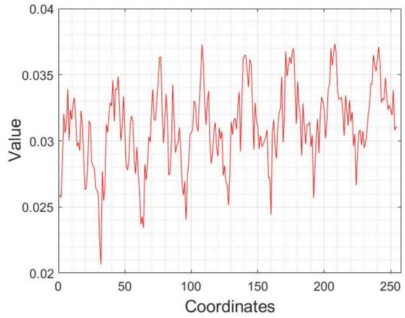

Fig. 11. Coefficients of the first principal component: Mandrill.

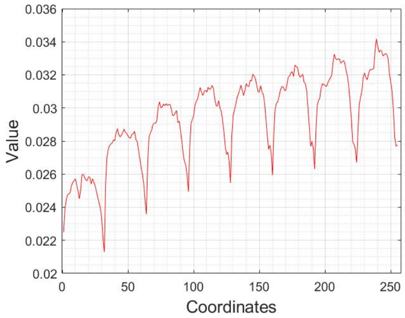

Fig. 12. Coefficients of the first principal component: Peppers.

The traditional methodology for the study of time series [22] is based on decomposing the series into several parts: trend, periodic variation, and other irregular fluctuations. In this paper, we applied the traditional methodology to the coefficients of the first principal components and analyzed the trend. Later, we analyzed the periodic fluctuations of the variable, in periods delimited by the size of the blocks in which we divided the images. It is important to point out that, after extracting the trend and cyclical variations from the series, we have a series of residual values, which may or may not be completely random.

Once the trend was eliminated, we analyzed the dependence between the observations. To analyze the seasonality of a series, we introduced the autocorrelation function. This function, for the $k \in \mathbb{N}$ value, measures the linear relationship between the values of the series spaced in k temporal units. If there is seasonality, the values separated from each other by intervals equal to the seasonal period must be correlated in some way. That is, the coefficient of autocorrelation for a delay equal to the seasonal period must be significantly different from 0.

Also, related to the autocorrelation function, we find the partial autocorrelation function. With the partial autocorrelation coefficient of order k, the correlation between the pair of values separated by that distance is calculated but eliminating the effect due to the correlation produced by the observations between them. Again, in this case, the presence of a value significantly different from zero will be indicating the probable presence of a seasonality factor for that delay value.

As can be seen in Figs. 7, 8, 9, 10, 11, and 12, where the images were decomposed in $2^h \times 2^h$ squares, with $h = 2$ and 3, all the figures seemed to have some component of period h. This suggested that there may be some relationship with the shape of the chosen blocks and, given that when we considered each of the 2^{2h} component vectors, the first 2^h pixels were adjacent with the next 2^h and so on up to 2^h times, most of the vectors were close to be periodic of period 2^h. Since the first principal components collect a large part of the characteristics of the vectors, it is plausible that they also reflect the periodicity of the vectors.

In this paper, in order to replace the coefficients of the first principal components, we eliminated the trend using low-degree polynomials, then analyzed the periodicity and replaced the $k \times k$ dimension vector with another whose components were periodic. After that, we added the trend to the periodic table and so we had already replaced the first components with their periodic versions. Finally, to evaluate the quality of the images reconstructed with the first periodic components, we found the value of PSNR and compared this value with the value of the PSNR when applying it to the principal components originally obtained.

III. Results

To illustrate the procedure and see the results, we will consider the image shown in Fig. 1. Next, we make a partition of this image and subdivide it into non-overlapping cells of size 8×8, $\mathbf{A}_{ij}$. With that we obtain $2^6 \cdot 2^6 = 4096$ blocks and each of these blocks will be a vector of observations. This matrix is given by (7). Later, we represent the coordinates of the first vectors of the base B', obtained as blocks of dimension $2^3 \times 2^3$ and are in $\mathbb{R}^{64}$. In Figs. 13, 14, 15, and 16, the coordinates of the first four principal components are shown with respect to the canonical basis. Although in fact the first eigenvalue is greater than the rest, what is appreciated is the possibility that these coefficients have periodic features by eliminating the possible trends that they have. For the first and fourth principal components, the trend is of the second degree, and for the second and third principal components, the trend is linear. There is a seasonality of delay 2^3 in the first four principal components, indicating that after eliminating the trend the coefficients of the principal components are approximately 2^3-periodic.

$$\mathbf{Image}_{64} = \begin{bmatrix} \mathbf{A}_{1,1} & \dots & \mathbf{A}_{1,64} \\ \vdots & \ddots & \vdots \\ \mathbf{A}_{64,1} & \dots & \mathbf{A}_{64,64} \end{bmatrix} \tag{7}$$

Figures 17, 18, 19, and 20 show eight repeated values periodically and added the respective trend. With the periodicity $2^k = 2^3$ and the considered trend, a great similarity between these principal components and the original principal components is obtained. Note that the original principal components and the principal components modified by periodicity practically overlap. This results in that the differences between the reconstructed images with the new vectors have to pick up the majority of the variability.

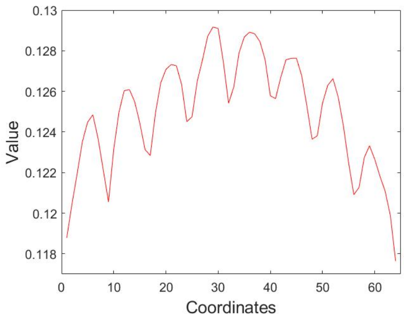

Fig. 13. Coefficients of the first principal component of Fig. 1 with respect to the canonical basis.

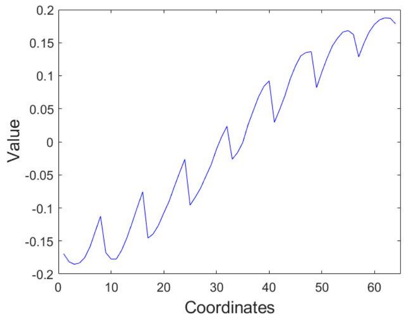

Fig. 14. Coefficients of second principal component of Fig. 1 with respect to the canonical basis.

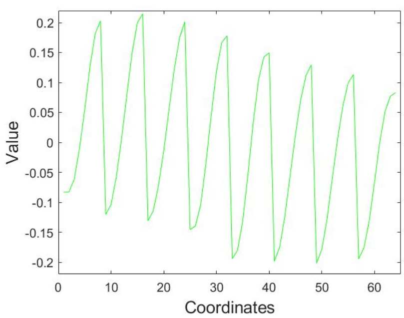

Fig. 15. Coefficients of the third principal component of Fig. 1 with respect to the canonical basis.

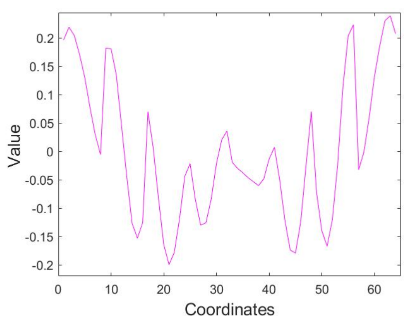

Fig. 16. Coefficients of the fourth principal component of Fig. 1 with respect to the canonical basis.

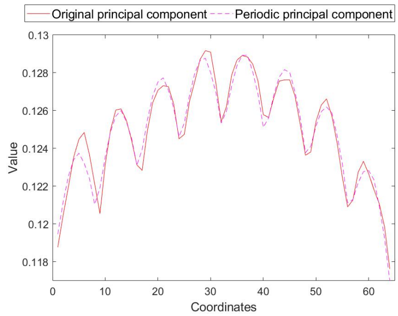

Fig. 17. Approximation by periodicity of Fig. 13

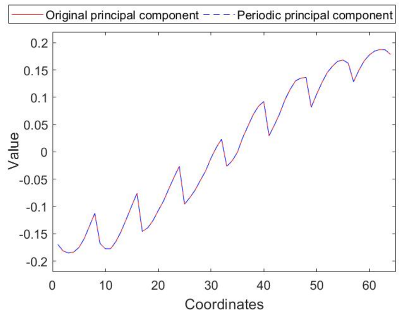

Fig. 18. Approximation by periodicity of Fig. 14

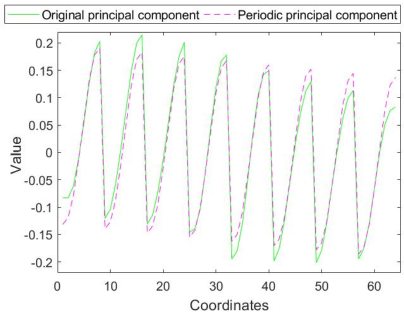

Fig. 19. Approximation by periodicity of Fig. 15

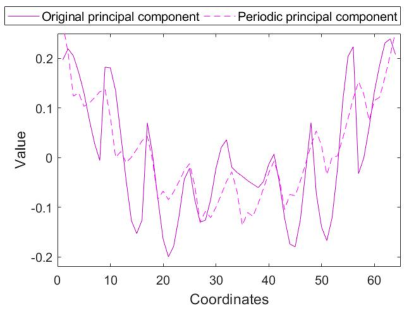

Fig. 20. Approximation by periodicity of Fig. 16

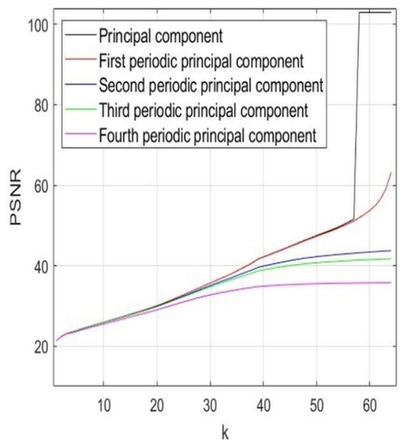

Fig. 21. PSNR of the first four original principal components and the first four principal components modified by periodicity.

Fig. 22. Approximation of the reconstructed image with 6 original principal components.

To analyze the quality of the reconstructions in Figs. 17, 18, 19, and 20, we have represented the value of the PSNR of the reconstructions of the image versus the number of principal components used for the reconstruction, and the PSNR of the reconstructions made with principal components modified by periodicity (see Fig. 21). Figures 22 and 23) show the reconstructions of Fig.1 with six original principal components and with the first six principal components altered by periodicity, respectively.

IV. Conclusions

Taking into account the results obtained in this paper, we can conclude that taking the principal components considered periodic and replacing them with their period plus a trend, we can say that these principal components are quite close to the reconstruction of the original image obtained using the original principal components. Therefore, vectors of length k^2 can be replaced by other vectors of length k and, consequently, the possibility of achieving improvements in the storage, processing, and transmission of the image is increased.

Fig. 23. Approximation of the reconstructed image with 6 periodic principal components.

Acknowledgment

This research has been supported by CEDIA-Ecuador (under the research project CEPRA XII-2018-13), Universidad de Las Americas, Quito, Ecuador (under the research project ERa.ERI.WHP.18.01), and Universidad Politecnica de Madrid, Spain.

References

[1] J. E. Jackson, *User's Guide to Principal Components*. John Wiley & Sons, 1991.

[2] K. I. Diamantaras and S. Y. Kung, *Principal Component Neural Networks: Theory and Applications*. John Wiley & Sons, 1996.

[3] I. T. Jolliffe, *Principal Component Analysis*, 2nd ed. Springer, 2002.

[4] R. A. Johnson and D. W. Wichern, *Applied Multivariate Statistical Analysis*, 6th ed. Pearson Education, 2007.

[5] W. Hernandez and A. Mendez, "Application of Principal Component Analysis to Image Compression," In *STATISTICS*, Türkmen Göksel, Ed. Rijeka: InTechOpen, 2018, Chapter 7, pp. 107-137. DOI: 10.5772/intechopen.75007. url: https://doi.org/10.5772/intechopen.75007

[6] H. Abdi and L. J. Williams, "Principal component analysis," *WIREs Computational Statistics*, vol. 2, no. 4, pp. 433-459, Jul./Aug. 2010.

[7] L. Huiqi and O. Chutatape, "Automatic location of optic disk in retinal images," *Proceedings 2001 International Conference on Image Processing (Cat. No.01CH37205)*, Thessaloniki, Greece, vol. 2, pp. 837-840, Oct. 7-10, 2001.

[8] P. Kumar Pandey, Y. Singh, and S. Tipathi, "Image Processing using Principle Component Analysis," *International Journal of Computer Applications*, vol. 15, no. 4, pp. 37-40, Feb. 2011.

[9] W. Hernandez, A. Mendez, and F. Ballesteros, "Image Noise Cancellation by Taking Advantage of the Principal Component Analysis Technique," *Proceedings of the 44th Annual Conference of the IEEE Industrial Electronics Society - IECON 2018*, Washington, DC, USA, pp. 3176-3181, Oct. 21-23, 2018.

[10] F. I. Bashir, A. A. Khokhar, and D. Schonfeld, "Real-Time Motion Trajectory-Based Indexing and Retrieval of Video Sequences," *IEEE Transactions on Multimedia*, vol. 9, pp. 58-65, Jan. 2007.

[11] K. Liu, Q. Du, H. Yang, and B. Ma, "Optical Flow and Principal Component Analysis-Based Motion Detection in Outdoor Videos," *EURASIP Journal on Advances in Signal Processing*, (2010) 2010: 680623. https://doi.org/10.1155/2010/680623

[12] S. M. Shiva Nagendra and M. Khare, "Principal component analysis of urban traffic characteristics and meteorological data," *Transportation Research Part D: Transport and Environment*, vol. 8, pp. 285-297, Jul. 2003.

[13] A. Lakhina, M. Crovella, and C. Diot, "Diagnosing Network-Wide Traffic Anomalies," *SIGCOMM'04 Proceedings of the 2004 conference on Applications, technologies, architectures, and protocols for computer communications*, Portland, Oregon, USA, pp. 219-230, Aug.30-Sep.3, 2004.

[14] R. Jiang-Tao, Ou Xiao-Ling, Yi Zhang, and Hu Dong-Cheng, "Research on network-level traffic pattern recognition," *Proceedings of The IEEE 5th International Conference on Intelligent Transportation Systems*, Singapore, pp. 500-504, Sep.3-6, 2002.

[15] V. Vitanis, R. Manka, D. Giese, H. Pedersen, S. Plein, P. Boesiger, and S. Kozerke, "High resolution three-dimensional cardiac perfusion imaging using compartment-based k-t principal component analysis," *Magnetic Resonance in Medicine*, vol. 65, pp. 575-587, Feb. 2011.

[16] F. Agahian, S. A. Amirshahi, and S. H. Amirshahi, "Reconstruction of reflectance spectra using weighted principal component analysis," *Color Research & Application*, vol. 33, pp. 360-371, Oct. 2008.

[17] F. Fang, X. He, H. Deng, Q. Cheng, J. Lu, M. Spraul, and Y. Yu, "Discrimination of metabolic profiles of pancreatic cancer from chronic pancreatitis by high-resolution magic angle spinning 1H nuclear magnetic resonance and principal components analysis," *Cancer Science*, vol. 98, pp. 1678-1682, Aug. 2007.

[18] T. Segreto, A. Simone, and R. Teti, "Principal component analysis for feature extraction and NN pattern recognition in sensor monitoring of chip form during turning," *CIRP Journal of Manufacturing Science and Technology*, vol. 7, pp. 202-209, May 2014.

[19] N. Sunita Devi and K. Hemachandran, "Face Recognition Using Principal Component Analysis," *International Journal of Computer Science and Information Technologies*, vol. 5, pp. 6491-6496, May 2014.

[20] H. Zheng-Hai, L. Wen-Juan, J. Wang, and T. Zhang, "Face recognition based on pixel-level and feature-level fusion of the top-level's wavelet sub-bands," *Information Fusion*, vol. 22, pp. 95-104, Mar. 2015.

[21] S. C. Ng, "Principal component analysis to reduce dimension on digital image," *Procedia Computer Science*, vol. 111, pp. 113-119, 2017.

[22] G. E. P. Box, G. M. Jenkins, G. C. Reinsel, and G. M. Ljung, *Time Series Analysis: Forecasting and Control*, 5th ed. Jhon Wiley & Sons, 2016.